

**Utah State University**

---

**From the Selected Works of Bela G. Fejer**

---

October 1, 2008

# Seasonal and longitudinal dependence of equatorial disturbance vertical plasma drifts

Bela G. Fejer, *Utah State University*

J. W. Jensen

S. Y. Su



Available at: [https://works.bepress.com/bela\\_fejer/53/](https://works.bepress.com/bela_fejer/53/)

## Seasonal and longitudinal dependence of equatorial disturbance vertical plasma drifts

Bela G. Fejer,<sup>1</sup> John W. Jensen,<sup>1,2</sup> and Shin-Yi Su<sup>3</sup>

Received 4 August 2008; revised 16 September 2008; accepted 22 September 2008; published 25 October 2008.

[1] We used equatorial measurements from the ROCSAT-1 satellite to determine the seasonal and longitudinal dependent equatorial  $F$  region disturbance vertical plasma drifts. Following sudden increases in geomagnetic activity, the prompt penetration vertical drifts are upward during the day and downward at night, and have strong local time dependence at all seasons. The largest prompt penetration drifts near dusk and dawn occur during June solstice. The daytime disturbance dynamo drifts are small at all seasons. They are downward near dusk with largest (smallest) values during equinox (June solstice); the nighttime drifts are upward with the largest magnitudes in the postmidnight sector during December solstice. During equinox, the downward disturbance dynamo drifts near sunset are largest in the eastern hemisphere, while the late night upward drifts are largest in the western hemisphere. The longitudinal dependence of the disturbance dynamo drifts is in good agreement with results from simulation studies. **Citation:** Fejer, B. G., J. W. Jensen, and S.-Y. Su (2008), Seasonal and longitudinal dependence of equatorial disturbance vertical plasma drifts, *Geophys. Res. Lett.*, 35, L20106, doi:10.1029/2008GL035584.

### 1. Introduction

[2] The morphology of the low latitude upper atmosphere has been studied extensively using mostly ground-based observations. These studies have indicated the occurrence of strong season and longitude dependent ionospheric effects associated with spatial variations of the ionospheric plasma drifts and thermospheric neutral winds. Over the last decade, measurements from several satellites have provided more detailed information on the global morphology of the low latitude ionosphere [e.g., Fejer *et al.*, 1995; Immel *et al.*, 2006; Fejer *et al.*, 2008].

[3] Low latitude ionospheric electric fields and currents often show very large departures from their quiet-time patterns during and after periods of enhanced geomagnetic activity. These perturbations, which have a broad range of time scales, are associated with high latitude electrodynamic disturbances. They can generally be explained as resulting from the combined effects of relatively short-lived prompt penetration electric fields driven by the solar wind-magnetosphere dynamo and longer lasting ionospheric

disturbance dynamo effects driven by enhanced energy and momentum deposition into the high latitude ionosphere [e.g., Fejer, 1997]. Recently, ROCSAT-1 and DMSP satellite measurements and complementary ground based observations have illustrated the complex global response of the low latitude ionosphere to large geomagnetic storms [e.g., Basu *et al.*, 2001; Lin *et al.*, 2001; Su *et al.*, 2003; Kil *et al.*, 2007; Heelis and Coley, 2007].

[4] In this study, we use vertical plasma drift measurements aboard ROCSAT-1 to examine for the first time the seasonal and longitudinal dependence of equatorial disturbance zonal electric fields. In the following section, we first briefly describe our database, and then discuss the prompt penetration and disturbance dynamo drift patterns derived from these measurements. Our results show the fundamental role of ionospheric conductance on the equatorial perturbation electric field drifts, and their opposite effects on the magnitudes of the prompt penetration and disturbance dynamo drifts.

### 2. Results and Discussion

[5] The ROCSAT-1 satellite made continuous plasma drift observations from mid-March 1999 to early June 2004 at an altitude of 600 km in a circular orbit with an inclination of 35° [e.g., Yeh *et al.*, 1999]. The errors on the equatorial vertical drifts were typically smaller than 10% when the ion density was larger than  $10^3 \text{ cm}^{-3}$  and the percentage of oxygen ions exceeds 85%. We have used 15-s averaged ROCSAT-1 vertical drifts within 5° of the dip equator. The data selection criteria are basically the same as described by Fejer *et al.* [2008], but with no restriction on the drift magnitude. These data were generally grouped into 1-hr four month seasonal bins representing and June Solstice (May–August), equinox (March–April, September–October), and December solstice (November–February). The average decimetric solar flux index of this database is about 150.

[6] We have studied the global climatological response of equatorial disturbance vertical plasma drifts using basically the methodology described by Fejer and Scherliess [1995]. In this procedure, we have determined the climatological hourly averaged disturbance drifts (except near sunset where we used half an hour averages) following idealized geomagnetic activity conditions, as specified by a time series of hourly  $AE$  indices, and then subtracted the corresponding season, solar cycle, and longitude dependent quiet time values.

#### 2.1. Prompt Penetration Drift Patterns

[7] Figure 1 shows the local time and season dependent longitudinally averaged prompt penetration drifts following

<sup>1</sup>Center for Atmospheric and Space Sciences, Utah State University, Logan, Utah, USA.

<sup>2</sup>Naval Air Warfare Center, China Lake, California, USA.

<sup>3</sup>Institute of Space Science and Center for Space and Remote Sensing Research, National Central University, Chung-Li, Taiwan.

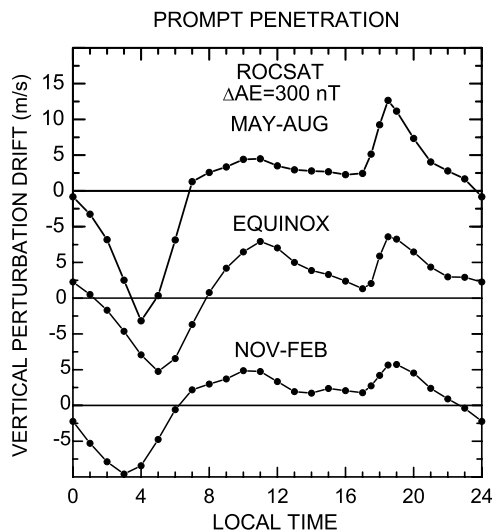


**Figure 1.** Seasonal dependence of longitudinally averaged equatorial prompt penetration vertical plasma drifts (positive upward) from ROCSAT-1 following a step function increase in the  $AE$  index by 300 nT.

a step function increase in geomagnetic activity normalized to  $\Delta AE = 300$  nT. The data points were obtained by averaging the perturbation drifts after increases in the hourly  $AE$  indices (centered at the times of measurements) larger than 125 nT, following at least 3 hours of relatively quiet conditions ( $AE < 300$  nT). The quiet time average  $AE$  was about 140 nT, and its average increase was about 240 nT. This binning criterion is identical to that used by *Fejer and Scherliess* [1995]. Following *Ahn et al.* [1992],  $\Delta AE = 300$  nT corresponds to an increase in the cross polar cap potential drop  $\Delta\Phi = 25$  kV.

[8] Figure 1 shows that, following a sudden increase in high latitude convection, the equatorial prompt penetration drifts are upward from about 0700 to 2300 LT, with peak values near 1100 and 1900 LT, and downward at night, with largest magnitudes between 0300 and 0500 LT. The daytime perturbation drifts are largest during equinox. Near sunrise and sunset the peak disturbance drifts have largest magnitudes during June solstice and smallest during December solstice. The drift reversal times occur earliest during the solstices and latest during equinox.

[9] The local time dependence of the prompt penetration drifts shown in Figure 1 is in good agreement with the season averaged values derived from Jicamarca radar observations [*Fejer and Scherliess*, 1995, 1997], and with results from global convection models [*Senior and Blanc*, 1984; *Spiro et al.*, 1988; *Fejer et al.*, 1990; *Peymirat et al.*, 2000]. Although our perturbation drifts are typical of only moderately disturbed conditions, their ratios to the  $AE$  index and polar cap potential drop are consistent with recent observations showing large prompt penetration drifts near sunrise and sunset during large magnetic storms [e.g., *Kil et al.*, 2007; *Heelis and Coley*, 2007]. Our results are also in good agreement with the perturbation electric field pattern associated with storm-time changes in the interplanetary electric field [*Kelley and Retterer*, 2008].

[10] Experimental [e.g., *Fejer*, 1986] and global convection model [e.g., *Tsunomura*, 1999; *Sazykin*, 2000] studies

indicate that near dusk and dawn the equatorial prompt penetration electric fields increase with decreasing solar flux. It has also been shown that the global ionospheric densities in the F-layer and TEC from high to equatorial latitudes have larger values in December solstice than in June solstice [e.g., *Rishbeth and Müller-Wodarg*, 2006; *Scherliess et al.*, 2008]. These results are consistent with the occurrence of largest prompt penetration drifts near sunrise and sunset during June solstice, as shown in Figure 1. We have not determined the prompt penetration drifts resulting from sudden decreases in geomagnetic activity since this requires the removal of longitude dependent disturbance dynamo effects. We expect these disturbance drift patterns to be similar to those in Figure 1, but with opposite polarities, as suggested by Jicamarca radar measurements associated with decreases in the  $AE$  indices and northward IMF  $B_z$  changes [*Fejer*, 1986; *Fejer and Scherliess*, 1995; *Kelley and Retterer*, 2008]. We have not been able to determine the longitudinal dependence of these prompt penetration drifts.

## 2.2. Disturbance Dynamo Drifts

[11] Figure 2 presents the season dependent longitude averaged disturbance drift patterns corresponding to nearly steady enhanced geomagnetic activity, and normalized  $\Delta AE = 300$  nT. In this case, the data were selected during periods when the hourly  $AE$  indices were larger than 200 nT for at least four hours, and the changes in the hourly indices were smaller than 125 nT, which are the binning criteria used by *Fejer and Scherliess* [1995]. Before normalization, these disturbance drifts corresponded to an average  $AE = 380$  nT (about 240 nT above the average quiet time value).

[12] Figure 2 shows small (on the order of the accuracy of our measurements) upward disturbance drifts between 0700 and 1700 LT during equinox and downward during the solstices. There are larger downward drifts near dusk and upward postmidnight drifts during all seasons. The downward perturbation drifts near dusk are largest during equinox and smallest during June solstice. The nighttime

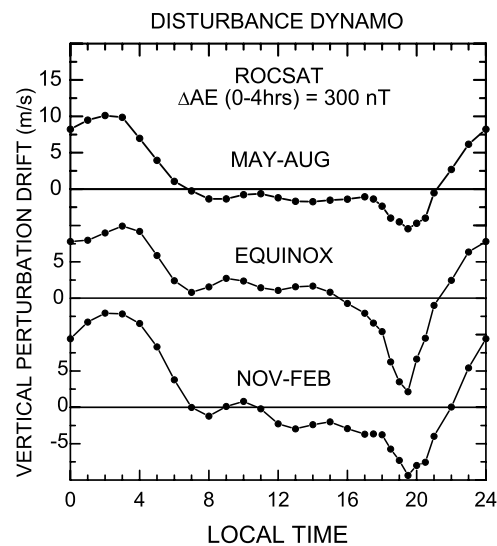


**Figure 2.** Seasonal dependence of longitudinally averaged equatorial disturbance dynamo vertical plasma drifts derived from ROCSAT-1 observations.

upward drifts are largest during December solstice, with peak values at about 0300 LT, and they have nearly identical magnitudes during June solstice and equinox. The local time and seasonal dependence of the disturbance dynamo drifts are largely anti-correlated with those of the prompt penetration drifts discussed earlier.

[13] The satellite perturbation drifts shown in Figure 2 are in good agreement with the corresponding season averaged empirical disturbance dynamo drifts derived from Jicamarca radar observations [Fejer and Scherliess, 1995; Scherliess and Fejer, 1997], and with theoretical results [Blanc and Richmond, 1980]. These radar data also indicate that, over the Peruvian equatorial region, the evening downward disturbance dynamo drifts during equinox are larger than during June solstice, and that the postmidnight upward drifts during these two seasons have comparable magnitudes [Fejer, 2002], which is again fully consistent with our satellite results. The equinox evening downward disturbance dynamo drifts measured by ROCSAT-1 increase with solar flux while the upward nighttime perturbations drifts are essentially unchanged [Jensen, 2007].

[14] Figure 3 presents the longitudinal dependence of the disturbance dynamo drifts during equinox obtained by averaging the residual drifts in  $120^\circ$  wide,  $60^\circ$  overlapping bins. The daytime perturbation drifts are small and variable and have low statistical significance. Figure 3 indicates that the largest downward (upward) perturbations near sunset (late night hours) occur in the eastern (western) hemisphere. It is interesting to note that the largest downward and upward perturbation drifts tend to occur at longitudes about  $180^\circ$  apart, which suggests that the equatorial ionospheric disturbance dynamo zonal electric fields are curl-free.

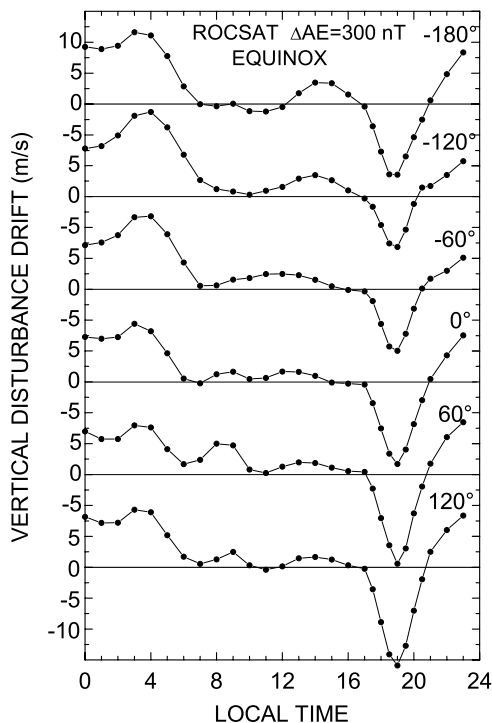


**Figure 3.** Longitudinal dependence of equatorial disturbance dynamo vertical plasma drifts during equinox.

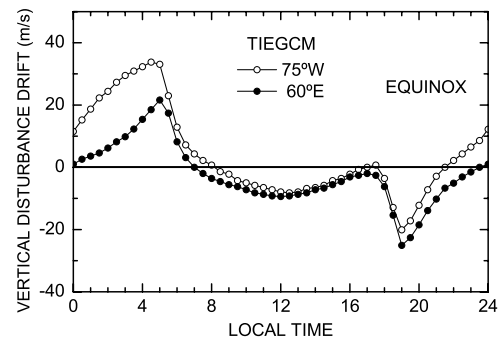


**Figure 4.** Equatorial disturbance dynamo vertical plasma drift patterns during equinox at two longitudes, derived from the TIEGCM simulations of Huang et al. [2005].

[15] Theoretical studies have pointed out that geomagnetic activity driven disturbance winds tend to charge the nighttime equatorial ionosphere positively, and that they produce largest electrodynamic effects in the postmidnight sector [e.g., Richmond et al., 2003]. Recently, Huang et al. [2005] used the Thermospheric Ionospheric Electrodynamic General Circulation Model (TIEGCM) to show that the electrodynamic effects of low latitude storm time winds during equinox have strong longitudinal dependence. Figure 4 presents the equatorial disturbance vertical drift patterns at  $75^\circ\text{W}$  and  $60^\circ\text{E}$  obtained by dividing the TIEGCM perturbation zonal electric fields from Huang et al. [2005] by the corresponding geomagnetic field strengths. These simulation disturbance electric fields were derived assuming moderate geomagnetic activity ( $\Delta K_p = 3$ ) constant for 5 days in order to reach a steady state. We note that the geomagnetic field strength is about 1.4 times stronger at  $60^\circ\text{E}$  than at  $75^\circ\text{W}$ .

[16] Figure 4 shows larger upward disturbance drifts at  $75^\circ\text{W}$  than at  $60^\circ\text{E}$  while the opposite is the case for the downward drifts near dusk. This longitudinal dependence is in good agreement with the experimental results shown in Figure 3. On the other hand, the simulation predicts a strong variation of the evening drift reversal time, which is not seen in our experimental data. The larger magnitude of the simulation drifts is most likely due to the assumption of longer lasting enhanced geomagnetic activity.

### 3. Summary

[17] We have determined the seasonal dependence of longitudinally averaged equatorial prompt penetration and disturbance dynamo vertical drifts. The prompt penetration drifts are mostly upward during the day and downward at night at all seasons. The peak daytime upward and nighttime downward prompt penetration drifts occur during June solstice. The general characteristics of the prompt penetration drift patterns derived from ROCSAT-1 measurements are consistent with earlier experimental and theoretical results. The disturbance dynamo drifts have small daytime values, they are downward near sunset where they increase with solar flux and have largest magnitudes during equinox and smallest during June solstice. The nighttime disturbance dynamo drifts are upward, do not change much with solar flux, and have the largest values near sunrise, especially during December solstice. The evening downward drifts



have largest values in the eastern hemisphere, and the nighttime upward drifts maximize in the western hemisphere. The satellite disturbance drift patterns are in good agreement with theoretical results.

[18] **Acknowledgments.** We thank N. Chapagain for help with the data. The work at Utah State was supported by the NASA Living With a Star (LWS) Program through grant NNX06AC44G, and by the Aeronomy Program of the National Science Foundation through grant ATM-0534038. The ROCSAT-1 data was processed under grant 93-NSPO(B)-IPEI-FA07-01 and S.-Y. Su was supported by the ROC NSC grant NSC93-211-M008-023-APS.

## References

- Ahn, B.-H., Y. Kamide, H. W. Kroehl, and D. J. Gorney (1992), Cross polar potential difference, auroral electrojet indices, and solar wind parameters, *J. Geophys. Res.*, *97*, 1345–1352.
- Basu, S., S. Basu, K. M. Groves, H.-C. Yeh, S.-Y. Su, F. J. Rich, P. J. Sultan, and M. J. Keskinen (2001), Response of the equatorial ionosphere in the South Atlantic region to the magnetic storm of July 15, 2000, *Geophys. Res. Lett.*, *18*, 3577–3580.
- Blanc, M., and A. D. Richmond (1980), The ionospheric disturbance dynamo, *J. Geophys. Res.*, *85*, 1669–1686.
- Fejer, B. G. (1986), Equatorial ionospheric electric fields associated with magnetospheric disturbances, in *Solar Wind-Magnetosphere Coupling*, edited by Y. Kamide and J. A. Slavin, pp. 519–545, Terra Sci., Tokyo.
- Fejer, B. G. (1997), The electrodynamics of the low-latitude ionosphere: Recent results and future challenges, *J. Atmos. Sol. Terr. Phys.*, *59*, 1465–1482.
- Fejer, B. G. (2002), Low latitude storm time ionospheric electrodynamics (2002), *J. Atmos. Sol. Terr. Phys.*, *64*, 1401–1408.
- Fejer, B. G., and L. Scherliess (1995), Time dependent response of equatorial ionospheric electric fields to magnetospheric disturbances, *Geophys. Res. Lett.*, *22*, 851–854.
- Fejer, B. G., and L. Scherliess (1997), Empirical models of storm time equatorial electric fields, *J. Geophys. Res.*, *102*, 24,047–24,056.
- Fejer, B. G., R. W. Spiro, R. A. Wolf, and J. C. Foster (1990), Latitudinal variation of perturbation electric fields during magnetically disturbed periods: 1986 SUNDIAL observation and model results, *Ann. Geophys.*, *8*, 441–454.
- Fejer, B. G., E. R. de Paula, R. A. Heelis, and W. B. Hanson (1995), Global equatorial ionospheric vertical plasma drifts measured by the AE-E satellite, *J. Geophys. Res.*, *100*, 5769–5776.
- Fejer, B. G., J. W. Jensen, and S.-Y. Su (2008), Quiet time equatorial  $F$  region vertical plasma drift model derived from ROCSAT-1 observations, *J. Geophys. Res.*, *113*, A05304, doi:10.1029/2007JA012801.
- Heelis, R. A., and W. R. Coley (2007), Variations in the low- and middle-latitude topside ion concentration observed by DMSP during superstorm events, *J. Geophys. Res.*, *112*, A08310, doi:10.1029/2007JA012326.
- Huang, C.-M., A. D. Richmond, and M.-Q. Chen (2005), Theoretical effects of geomagnetic activity on low-latitude ionospheric electric fields, *J. Geophys. Res.*, *110*, A05312, doi:10.1029/2004JA010994.
- Immel, T. J., E. Sagawa, S. L. England, S. B. Henderson, M. E. Hagan, S. B. Mende, H. U. Frey, C. M. Swenson, and L. J. Paxton (2006), Control of equatorial ionospheric morphology by atmospheric tides, *Geophys. Res. Lett.*, *33*, L15108, doi:10.1029/2006GL026161.
- Jensen, J. W. (2007), Climatology of middle and low-latitude  $F$ -region plasma drifts from satellite measurements, Ph.D. thesis, Utah State Univ., Logan.
- Kelley, M. C., and J. Retterer (2008), First successful prediction of a convective equatorial ionospheric storm using solar wind parameters, *Space Weather*, *6*, S08003, doi:10.1029/2007SW000381.
- Kil, H., S.-J. Oh, L. J. Paxton, Y. Zhang, S.-Y. Su, and K.-W. Min (2007), Spike-like change of the vertical  $E \times B$  drift in the equatorial region during very large geomagnetic storms, *Geophys. Res. Lett.*, *34*, L09103, doi:10.1029/2007GL029277.
- Lin, C. S., H. C. Yeh, and S.-Y. Su (2001), ROCSAT-1 satellite observations of magnetic anomaly density structures during the great magnetic storm of July 15–16, 2000, *Terr. Atmos. Oceanic Sci.*, *12*(3), 567–582.
- Peymirat, C., A. D. Richmond, and A. T. Koba (2000), Electrodynamical coupling of high and low latitudes: Simulations of shielding/overshielding effects, *J. Geophys. Res.*, *105*, 22,991–23,003.
- Richmond, A. D., C. Peymirat, and R. G. Roble (2003), Long-lasting disturbances in the equatorial ionospheric electric field simulated with a coupled magnetosphere-ionosphere-thermosphere model, *J. Geophys. Res.*, *108*(A3), 1118, doi:10.1029/2002JA009758.
- Rishbeth, H., and I. C. F. Müller-Wodarg (2006), Why is there more ionosphere in January than in July? The annual asymmetry in the  $F$ -2 layer, *Ann. Geophys.*, *24*, 2393–3311.
- Sazykin, S. (2000), Theoretical studies of penetration of magnetospheric electric fields to the ionosphere, Ph.D. dissertation, 292 pp., Utah State Univ., Logan.
- Scherliess, L., and B. G. Fejer (1997), Storm time dependence of equatorial disturbance dynamo zonal electric fields, *J. Geophys. Res.*, *102*, 24,037–24,046.
- Scherliess, L., D. C. Thompson, and R. W. Schunk (2008), Longitudinal variability of low-latitude total electron content: Tidal influences, *J. Geophys. Res.*, *113*, A01311, doi:10.1029/2007JA012480.
- Senior, C., and M. Blanc (1984), On the control of magnetospheric convection by the spatial distribution of ionospheric conductivities, *J. Geophys. Res.*, *89*, 261–284.
- Spiro, R. W., R. A. Wolf, and B. G. Fejer (1988), Penetration of high-latitude electric fields effects to low latitudes during SUNDIAL 1984, *Ann. Geophys.*, *6*, 39–50.
- Su, S.-Y., C. K. Chao, H. C. Yeh, and R. A. Heelis (2003), Observations of shock impact, disturbance dynamo effect, and a midlatitude large-density depletion at 600 km altitude on the 17 April 2002 storm day, *J. Geophys. Res.*, *108*(A8), 1310, doi:10.1029/2002JA009752.
- Tsunomura, S. (1999), Numerical analysis of global ionospheric current system including the effect of the equatorial enhancement, *Ann. Geophys.*, *17*, 692–706.
- Yeh, H.-C., S.-Y. Su, Y. C. Yeh, J. M. Wu, R. A. Heelis, and B. J. Holt (1999), Scientific mission of the IPEI payload onboard ROCSAT-1, *Terr. Atmos. Oceanic Sci.*, *suppl.*, 19–42.

B. G. Fejer and J. W. Jensen, Center for Atmospheric and Space Sciences, Utah State University, Logan, UT 84322, USA. (bfejer@cc.usu.edu)  
S.-Y. Su, Institute of Space Science, National Central University, 300 Chung-Da Road, Chung-Li, 32054 Taiwan.